

Suzaku Observation of the Radio Halo Cluster Abell 2319

– Hard X-ray Properties and Gas Dynamics –

Motokazu Takizawa¹, Chika Sugawara², and Kazuhiro Nakazawa³

¹ Department of Physics, Yamagata University, Kojirakawa-machi 1-4-12, Yamagata 990-8560, Japan

² Graduate School of Science and Engineering, Yamagata University, Kojirakawa-machi 1-4-12, Yamagata 990-8560, Japan

³ Department of Physics, The University of Tokyo, 7-3-1 Hongo, Bunkyo-ku, Tokyo 113-0033, Japan

E-mail(MT): takizawa@sci.kj.yamagata-u.ac.jp

ABSTRACT

We present the results of Suzaku observation of the radio halo cluster Abell 2319. We confirm that the line-of-sight velocities of the intracluster medium in the observed region are consistent with those of the member galaxies of entire A2319 and A2319A subgroup for the first time, though any velocity difference within the region is not detected. On the other hand, we do not find any signs of gas motion relevant to A2319B subgroup. Hard X-ray emission from the cluster is clearly detected, but its spectrum is likely thermal. Assuming a simple single temperature model for the thermal component, we find that the upper limit of the non-thermal inverse Compton component becomes $2.6 \times 10^{-11} \text{ erg s}^{-1} \text{ cm}^{-2}$ in the 10-40 keV band, which means that the lower limit of the magnetic field is $0.19 \mu\text{G}$ with the radio spectral index 0.92. Considering that the lack of a significant amount of very hot ($\sim 20 \text{ keV}$) gas and the strong bulk flow motion, it is more likely that the relativistic non-thermal electrons responsible for the radio halo are accelerated through the intracluster turbulence rather than the shocks.

KEY WORDS: galaxies: clusters: individual (Abell 2319) — X-rays: galaxies: clusters

1. Introduction

Diffuse non-thermal synchrotron radio emission is found in a significant fraction of galaxy clusters, which indicates that there exist both the relativistic electrons and magnetic field as well as the thermal intracluster medium (ICM) in the intracluster space. Although the origin of these non-thermal electrons is still unclear, some connections of radio halos and relics with dynamical motion of ICM are reported. Abell 2319 is one of the most well-known examples of merging clusters with a giant radio halo (Feretti et al. 1997). Two subgroups, A2319A and A2319B, are recognized in radial velocity distribution of the member galaxies, which suggests that the velocity difference between them is almost 3000 km s^{-1} (Oegerle et al. 1995). Observations in the hard X-ray band are performed by Beppo-SAX, RXTE, and Swift-BAT, any of which do not report firm detection of non-thermal components. In this paper, we present Suzaku observation of the Abell 2319 cluster to investigate dynamical status of the ICM and hard X-ray properties (Sugawara et al. 2009).

2. Observations

We observed the central region of Abell 2319 with Suzaku on 2006 October 27-30 for an exposure time of 100 ks.

The field of view (FOV) of Suzaku XIS, and that of HXD PIN in which the throughput of the fine-collimator becomes 50 % are shown in a ROSAT PSPC image (figure 1). An approximate position of the A2319B subgroup is also shown. The observation was performed at HXD nominal pointing. The XIS was operated in the normal full-frame clocking mode.

3. Results

We divide XIS FOV into 11 regions shown in figure 2 and perform spectral analysis for each region. We use Doppler-shifted He like Fe $K\alpha$ lines (6.679 keV) and H like Fe $K\alpha$ line (6.964 keV) to determine ICM line-of-sight (LOS) velocities. Therefore, if the ICM motion is $\sim 1000 \text{ km s}^{-1}$, we should resolve the energy shift of only $\sim 22 \text{ eV}$. This is a challenging task considering that energy resolution of XIS is 130 eV (FWHM). To measure an energy scale of XIS accurately, we make a gain correction with Mn $K\alpha$ lines of the calibration sources on each XIS sensor. We fit spectra of each XIS sensor with APEC model. Figure 3 shows LOS velocities of the ICM for the regions presented in figure 2, where upper, middle, and lower horizontal lines represent the mean LOS velocities of the member galaxies for the A2319B subgroup, entire A2319, and A2319A subgroup, respectively. Basically,

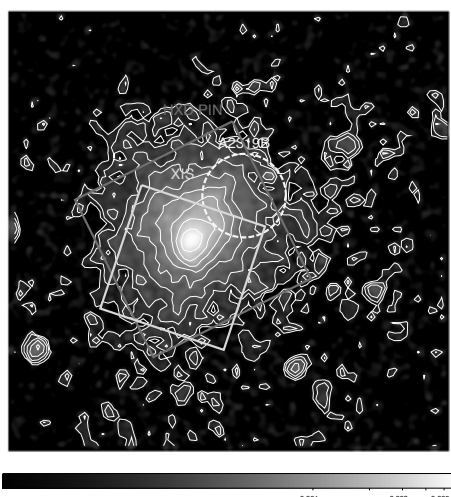


Fig. 1. ROSAT PSPC image of the Abell 2319 overlaid with field of view of Suzaku XIS CCDs, and that of HXD PIN in which the throughput of the fine-collimator becomes 50%. An approximate position of the subgroup A2319B is also represented by dotted circle.

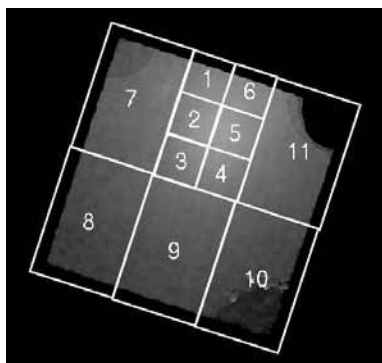


Fig. 2. Region numbers used in measurement of the line-of-sight velocity of the ICM in figure 3.

the obtained ICM velocities lie between those of entire A2319 and A2319A. No significant velocity difference is detected within the observed region.

We perform joint spectral analysis of PIN and XIS to investigate hard X-ray properties. We use a spectral model of single temperature APEC plus power-law model ($1kT + PL$). A photon index of the power-law component is fixed to 1.92 assuming that it is emitted via inverse Compton process of cosmic microwave background (CMB) from the same electron population that radiates synchrotron radio. Figure 4 show the spectral fit results. In the joint spectrum analysis of PIN and XIS, non X-ray background (NXB) and cosmic X-ray background (CXB) components are fluctuated at the 90 % confidence level of the systematic uncertainty (4.5% and 18% for NXB and CXB, respectively). This causes the changes of the best-fit parameters in the fits and gives us the systematic errors. Including both the statistical

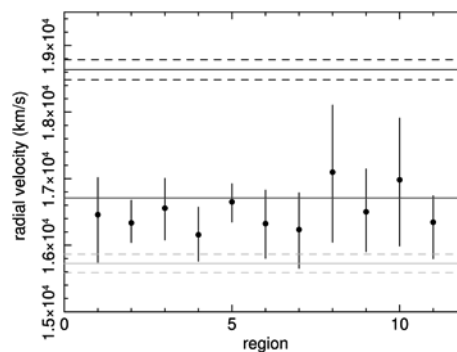


Fig. 3. Line-of-sight velocities of the ICM for the regions presented in figure 2. Upper, middle, and lower horizontal lines show the mean line-of-sight velocities of the member galaxies for the A2319B subgroup, entire A2319, and A2319A subgroup, respectively.

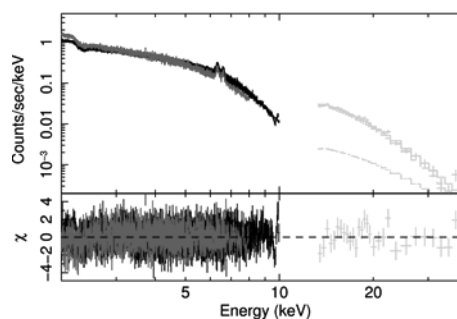


Fig. 4. The wide band spectrum of the A2319 fitted with the $1kT + PL$ model with a photon index 1.92. The best fit model is presented in dashed histograms. Thermal and power-law components are independently presented as dashed histograms for HXD. Only thermal component is presented for XIS.

errors and systematic ones of CXB and NXB, we derive an upper limit of a power-law component in 10-40 keV at the 90 % confidence level. The resultant upper limit becomes $2.6 \times 10^{-11} \text{ erg s}^{-1} \text{ cm}^{-2}$. Assuming that this hard X-ray component is emitted via inverse Compton scattering of CMB photons by the electron population responsible to the synchrotron radio halo, this upper limit gives us the lower limit of the magnetic field strength of $0.19 \mu\text{G}$.

M. T. was supported in part by a Grant-in-Aid from the Ministry of Education, Science, Sports, and Culture of Japan (19740096).

References

- Feretti L. et al. 1997 *New Astronomy*, 2, 501
- Oegerle W. R. et al. 1995 *AJ.*, 110, 32
- Sugawara C. et al. 2009 *PASJ.*, in press (arXiv:0909.1358)